PART III

LABORATORY ASTROPHYSICS STUDIES OF DIB CARRIER (RELATED) CANDIDATES

The Diffuse Interstellar Bands
Proceedings IAU Symposium No. 297, 2013
J. Cami & N. L. J. Cox, eds.

doi:10.1017/S1743921313015949

Laboratory Electronic Spectra of Carbon Chains and Rings

L. N. Zack and J. P. Maier

Department of Chemistry, University of Basel,
Klingelbergstrasse 80, CH-4056, Basel, Switzerland
email: j.p.maier@unibas.ch

Abstract. Carriers of the diffuse interstellar bands (DIBs) cannot be definitively identified without laboratory spectra. Several techniques, including matrix isolation, cavity ringdown spectroscopy, resonance enhanced multiphoton ionization, and ion trapping, have been used to measure the electronic spectra of carbon chains and their derivatives. The gas-phase laboratory spectra could then be compared to the astronomical data of known DIBs. The choice of molecules studied in the gas phase depends on the presence of strong electronic transitions at optical wavelengths, the lifetimes of excited electronic states, and chemical feasibility in diffuse astrophysical environments. Collisional-radiative rate models have also be used in conjunction with laboratory spectra to predict absorption profiles under interstellar conditions.

Keywords. astrochemistry, methods: laboratory, techniques: spectroscopic, ISM: molecules, ISM: clouds

---

Over the last several decades, many different computational and laboratory-based approaches have been applied to the problem of identifying the carriers of the diffuse interstellar bands (DIBs). Early explanations for these broad absorptions suggested that they originated from either dust or predissociated molecules. However, the identification of numerous carbon-containing species in dense clouds via mm-wave astronomy led to a more rational approach in the search for likely carriers of DIBs. Many of the detected species are polar carbon chains terminated by H, N, or O atoms (see: http://www.astro.uni-koeln.de/cdms/molecules). This prompted the suggestion that the non-polar carbon chains containing up to a handful of atoms were potential candidates because non-radiative processes, rather than predissociation, could lead to broadening of the absorptions (Douglas 1977). However, only the electronic spectra of C_2 and C_3 were known at that time, and gas-phase spectra of the longer carbon chains were required for comparison with DIB data. Thus, we tasked ourselves the goal of obtaining the spectra of these species and their derivatives.

Several methods were developed to measure electronic spectra of hitherto unknown polyatomic species, particularly those containing a carbon backbone (chain or ring), as well as their ions. The first approach relied on the detection of fluorescence from the excited electronic states and as a result, the spectra of over a hundred organic open-shell cations could be measured (Nagarajan & Maier 2010, and references therein). However, as fluorescence from the excited electronic states is an exception rather than rule for large cations, other techniques were required. This led to the use of cavity ringdown spectroscopy using pulsed and cw lasers, resonant two-color, two-photon ionization, and degenerate four wave mixing. In addition, for cations the use of ion traps and two-photon excitation-dissociation schemes have been successfully added to the armory of techniques (e.g. Jochnowitz & Maier 2008a, and references therein).

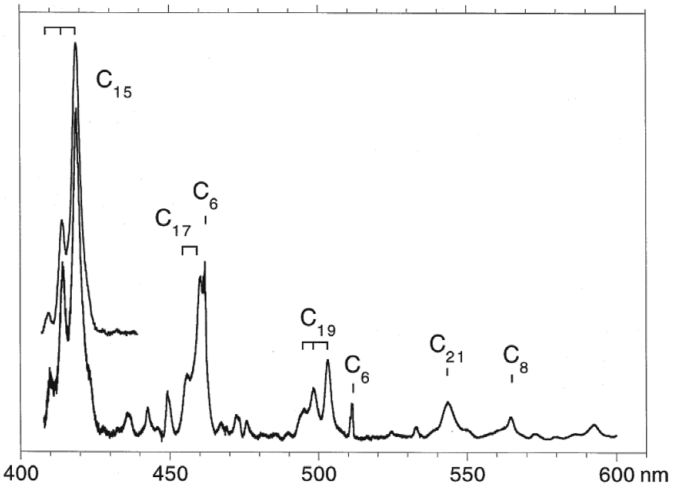

Figure 1. Absorption spectra of several linear carbon chains lying in the DIB region recorded in a 6 K neon matrix. For C_6 and C_8, the $^3\Sigma_u^- \leftarrow X\,^3\Sigma_g^-$ transition is shown, while the C_{15}, C_{17}, C_{19}, and C_{21} features belong to $^1\Sigma_u^+ \leftarrow X\,^1\Sigma_g^+$ transitions. (Taken from Wyss *et al.* 1999.)

In order to initially locate the wavelength of the electronic transitions, we developed an approach to measure the spectra of these species in neon matrices using mass-selected ions. This method proved successful, allowing us to observe these electronic absorptions for the first time. An example of these data is shown in Fig. 1, which displays the spectra of linear chains with an odd-number of carbon atoms absorbing at visible wavelengths, i.e the DIB range ($\approx 4400-9500$ Å). Many of the spectra were measured individually using mass selection of the anions, followed by photodetachment (Wyss *et al.* 1999). Absorption wavelengths of the anions were also located. Similar measurements were made on neutral, cationic, and anionic chains capped by one or two hydrogen atoms. The $C_{2n}H$ species are polar, open-shell molecules with absorptions in the visible that redshift as the size of the system increases. The $HC_{2n}H$ species absorb in the UV and would have to be very large to fall in the DIB range; however, their cations, $HC_{2n}H^+$, within a certain size, possess transitions in the visible region. This aspect is illustrated in Fig. 2 where the wavelength of the origin band of acetylenic chains is plotted as a function of chain length. But, the matrix data cannot be used for direct comparison to DIBs due to shifts of 10 – 30 Å relative to the gas phase. The uncertainty is small enough, however, to look for the transition with laser techniques.

In order to illustrate this point, the electronic absorption spectrum of C_{60}^+ recorded in a 6 K neon matrix is shown in Fig. 3 (Fulara *et al.* 1993). The absorption at 9645 Å is the origin band, and the subsidiary structure is probably due to solid state effects. The second band around 9400 Å is the absorption from the lowest level in the ground state to a vibrational level in the excited electronic state. The data were subsequently used for comparison with DIB measurements in this region (shown in upper trace of Fig. 3) and led the authors to propose that C_{60}^+ is the carrier of the two DIB absorptions (Foing & Ehrenfreund 1994). In view of the uncertainty in the neon matrix shift, this conclusion remains unsettled and awaits a gas-phase laboratory measurement.

The electronic absorption spectra of C_4, C_5, C_6H, and C_8H were recorded in the gas phase using either cavity ringdown or two-color resonant ionization techniques (Jochnowitz & Maier 2008b, and references therein). These molecules were prepared in situ using pulsed supersonic expansions coupled with a discharge or laser ablation source. Because

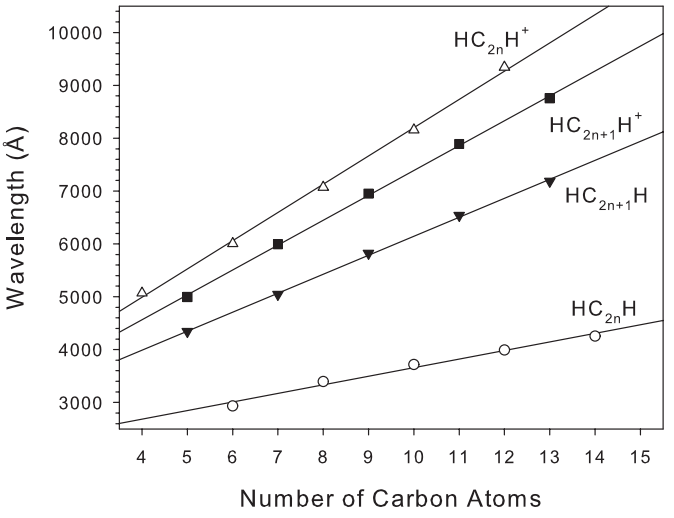

Figure 2. Approximate linear dependence of the origin band wavelengths on the number of carbon atoms for neutral and cationic acetylenic chain species. The $A^2\Pi \leftarrow X^2\Pi$ transitions of $HC_{2n}H^+$ and $HC_{2n+1}H^+$, the $A^1\Delta_u \leftarrow X^1\Sigma_g^+$ transition of $HC_{2n}H$, and the $A^3\Sigma_u^- \leftarrow X^3\Sigma_g^-$ transition of $HC_{2n+1}H$ are shown.

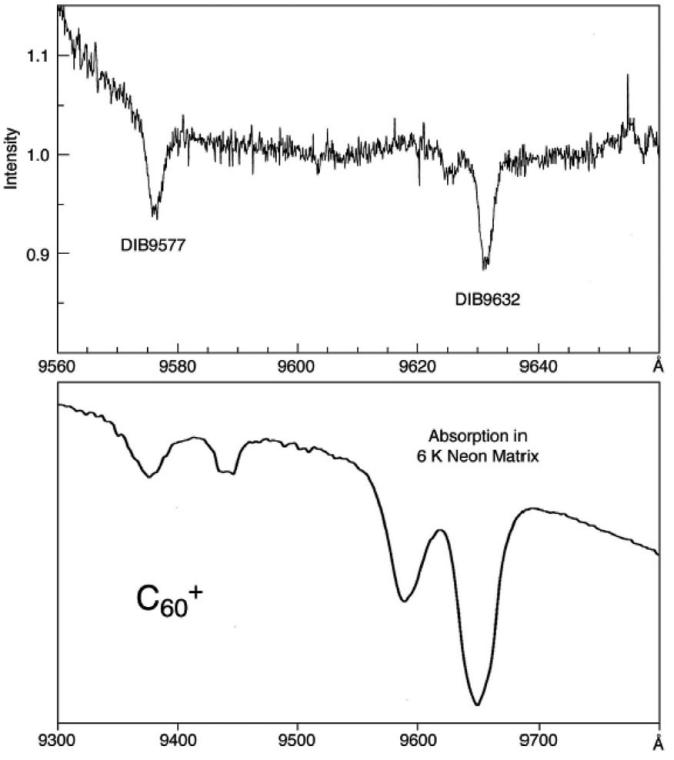

Figure 3. Astronomical spectrum (top) of two DIBs (Foing & Ehrenfreund 1994) compared to the 6 K neon matrix spectra (bottom) of the $^2E_{1g} \leftarrow X\,^2A_{1u}$ transition of the C_{60}^+ cation (Fulara *et al.* 1993). (The wavelength axes for the two spectra are not on the same scale.)

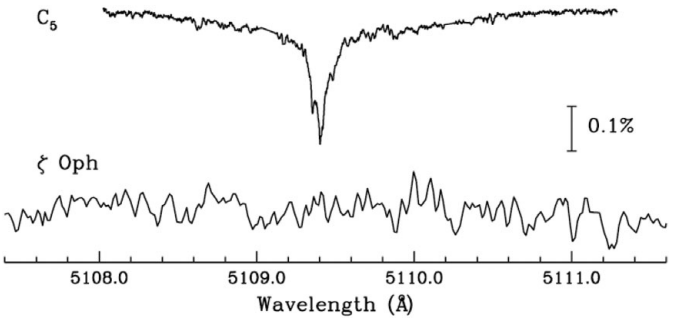

Figure 4. Comparison of the laboratory spectrum (top) of the origin band in the $^1\Pi_u \leftarrow X\,^1\Sigma_g^+$ electronic transition of C_5 at 80 K with an astronomical observation (bottom) towards ζ Oph (Maier *et al.* 2002).

they have absorptions at visible wavelengths, attempts were made to detect C_4 and C_5 in diffuse clouds, but only upper limits to the column density could be determined (Maier *et al.* 2002). Figure 4 shows the comparison of the laboratory and astronomical data for the origin band of the $^1\Pi_u \leftarrow X\,^1\Sigma_g^+$ electronic transition of C_5.

Additional comparisons were made for C_nH species, polyacetylene and cyanopolyacetylene cations, and carbon anion chains. None of their absorptions could be unambiguously correlated with a DIB absorption, although some intriguing similarities were noted. In the cases of the anions C_7^- and H_2CCC^- the origin bands and several additional transitions were close in wavelength (within 2 Å) to weaker DIBs (McCall *et al.* 2000, 2002). The origin band of the $A^2\Pi_g \leftarrow X\,^2\Pi_u$ transition of $NCCCCN^+$ at 80 K is shown in the left panel of Fig. 5; the double-humped profile of the origin band is practically superimposable with that of a DIB except for a 1 Å shift (Motylewski *et al.* 2000). Also displayed in Fig. 5 (right panel) are the rotational profiles of this transition over the temperature range 3 – 150 K. The C_7^-, H_2CCC^-, and $NCCCCN^+$ cases may be relevant to the recent suggestion that molecules in diffuse clouds are possibly surrounded by layers of hydrogen molecules (Bernstein *et al.* 2013), which would lead to small shifts in the band positions.

Cyclic C_{18}, which was measured in the gas-phase in the laboratory using a resonance enhanced ionization approach, provides another intriguing example, as illustrated in Fig. 6. Here, rotational profiles for the origin band of the lowest electronic transition are shown at 100, 50, and 20 K, reflecting changes in the residual populations of the low-frequency vibrational modes (left panel; Maier *et al.* 2006). The profiles are almost superimposable with DIBs measured at comparable resolution, albeit at different wavelengths (right panel; Sarre *et al.* 1995). The similarities between the simulated profiles and DIB data make it appear feasible that carbon rings with up to 100 atoms, possibly containing hydrogen or nitrogen and including their cations, with large oscillator strengths may be the carriers of the DIBs shown.

As part of the search for the signatures of C_4 and C_5 in diffuse clouds, the 4056 Å absorption corresponding to the $^1\Pi_u \leftarrow X\,^1\Sigma_g^+$ transition of C_3 was also targeted using the Canada-France-Hawaii telescope on Mauna Kea (Maier *et al.* 2001). The astronomical spectra unambiguously identified C_3 in diffuse clouds, as shown in Fig. 7, with the intensity distribution of the peaks implying a dominant rotational temperature of 80 K. The successful identification of C_3 has imposed certain requirements for other potential carriers. First, the molecule must have a strong electronic transition in the DIB range. Additionally, the product of the column density and oscillator strength must be sufficient to correspond to the more prominent DIBs, with equivalent widths of 0.1 Å. Thus, if one takes a column density of 10^{11} cm^{-2} as typical, based on upper limits $\leqslant 10^{12}$ cm^{-2} inferred

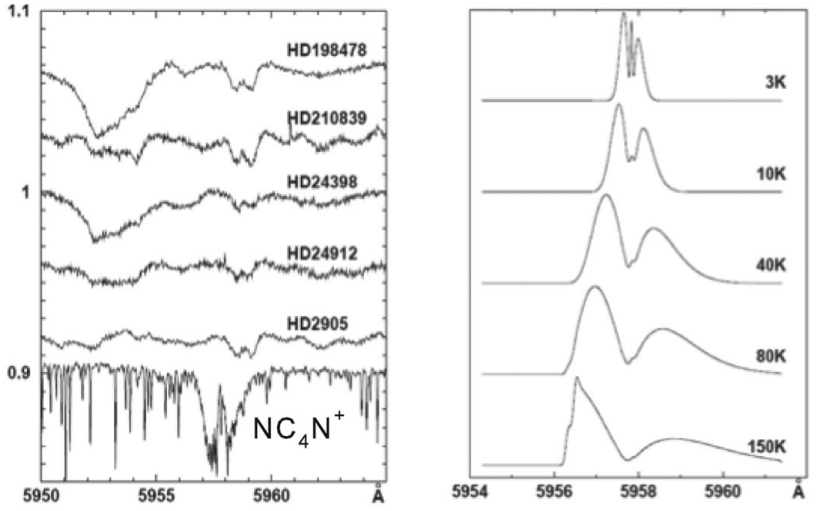

Figure 5. The origin band of the $A\,^2\Pi_g \leftarrow X\,^2\Pi_u$ transition of $NCCCCN^+$ measured at 80 K in the laboratory compared to DIB absorptions (left). If the temperature is varied from 3 – 150 K, the rotational profile changes in both shape and wavelength (right; Motylewski *et al.* 2000).

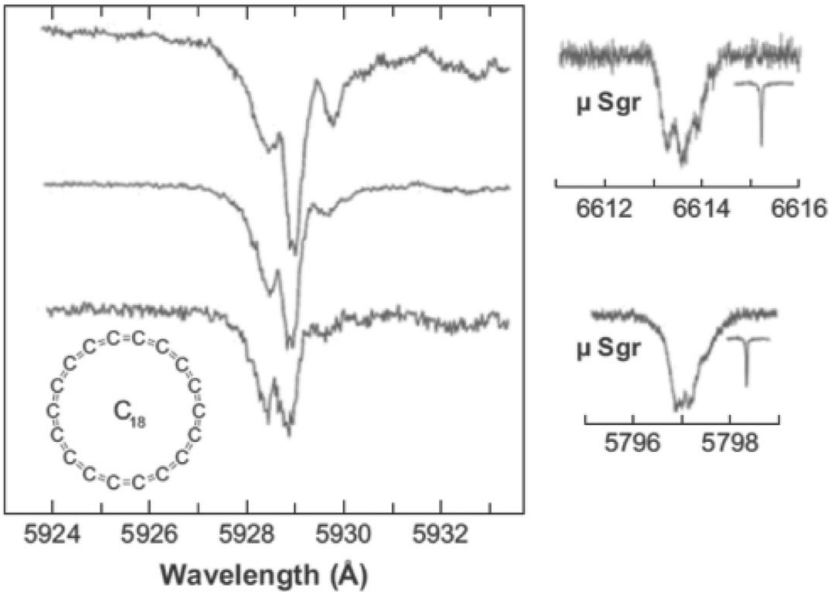

Figure 6. Rotational profile of the origin band in the lowest electronic transition of cyclic C_{18} at 100, 50, and 20 K (top, middle, and bottom traces, respectively) measured in the laboratory. The right panel shows two DIB absorptions taken towards μ Sgr with similar profiles, although at different wavelengths (Sarre *et al.* 1995).

from the comparison of gas-phase electronic spectra with DIB data (Motylewski *et al.* 2000), an oscillator strength on the order of unity is a necessary requirement. Using the $^1\Sigma_u^+ \leftarrow X\,^1\Sigma_g^+$ transition of C_{2n+1} as an example, the C_3 absorption lies around 1600 Å, whereas that of C_{15} is redshifted to around 4200 Å, as seen in Fig. 1. Thus, although these species satisfy the above criteria, only a few will have transitions falling within the DIB range (namely, C_{17}, C_{19}, ...) and have the required large oscillator strengths.

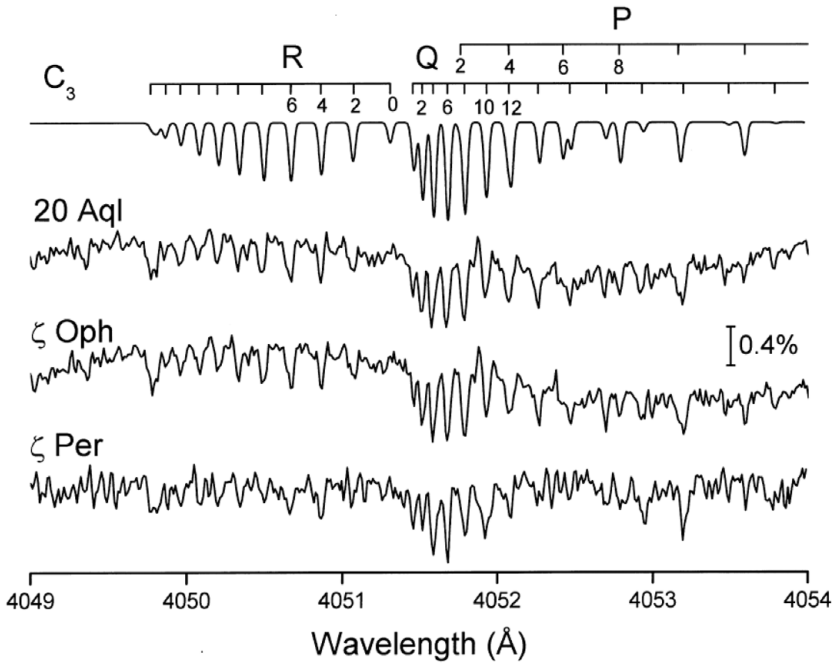

Figure 7. Origin band of the $^1\Pi_u \leftarrow X\,^1\Sigma_g^+$ transition of C_3 at 80 K (top trace) compared to the absorptions through diffuse clouds (Maier *et al.* 2001).

Corresponding isoelectronic systems, including cations, that terminate in nitrogen or oxygen atoms can also fulfill these requirements. Uncertainty remains, however, regarding the lifetimes of their excited $^1\Sigma_u^+$ states. If the lifetimes are shorter than around 100 fs, Heisenberg's lifetime broadening would lead to absorptions with FWHM >20 Å, which is too large to be associated with with the typical DIB FWHM $\approx 0.1-1$ Å. Unfortunately, this property is molecule specific and cannot be predicted using current theory.

The importance of lifetime broadening is illustrated by considering the C_4 and C_5 species. The $^1\Pi_u$ excited state of the C_5 transition shown in Fig. 4 is found to have a lifetime of around 10 ps, as established by time-resolved excitation-ionization studies (Boguslavskiy & Maier 2006), corresponding to an ≈ 1 Å FWHM for the absorption band. Thus, even a molecule as small as C_5 can have fast intramolecular processes for the excited electronic state. However, other species comparable in size, e.g. HC_4H^+, have excited state lifetimes of around 80 ns, allowing the rotational structure of their electronic transitions to be resolved. Recent laboratory studies using a resonance enhanced ionization scheme with ps lasers show the excited electronic states of C_6-C_9 to have lifetimes less than 30 ps.

The previous discussion has focused on transitions to the lowest excited electronic state, but those to higher ones are also relevant. In Fig. 2 only transitions to the lowest excited electronic state are shown, illustrating that for a particular homologous series only a certain number of molecules will absorb in the DIB range. However, these types of species have transitions to higher-energy states which will eventually shift into the 4400–9000 Å window when the system becomes large enough. It was previously assumed that these transitions could not be considered for DIB comparisons because they were expected to have lifetimes in the fs range, making their absorptions too broad to be relevant for DIB considerations. However, recent measurements on polyacetylene cations held in a radio frequency trap led to unexpected results. In this case, the internal temperature

of the mass-selected ions was equilibrated to ≈ 20 K by collisions with cryogenically-cooled helium (Rice *et al.* 2010) and the absorptions were recorded using a two photon excitation–dissociation scheme. Surprisingly, not all of the origin bands for transitions to higher excited electronic states were too broad to be excluded. In some cases, widths of only 1 – 2 Å were observed, making them relevant for consideration, although no matches with DIBs were found. Nonetheless, it is important to note that, as for the lowest excited electronic states, it is a priori not evident whether the absorptions are too broad or not.

The significant conclusion from these laboratory and astronomical comparisons is that although molecules such as the C_5, C_6H, etc. chains are undoubtedly present in the diffuse clouds and in fact, C_3H and C_4H have been directly detected by radio astronomy, these sorts of molecules cannot result in DIB absorptions of 0.1 EW intensity. Thus, the proposition that "...the absorbing species are long chain carbon molecules, C_n where n may lie in the range 5–15" (Douglas 1977) is now excluded. Generally carbon chains up to a dozen atoms, their ions, and simple derivatives containing H or N are not responsible for the typical DIBs, as the product of their likely column densities ($\approx 10^{11} - 10^{12}$ cm^{-2}) and transition moments would lead to mÅ EWs.

Another way of approaching the DIB problem from a laboratory standpoint is to not target a specific molecule. One can apply a discharge to supersonically-expanding gas mixtures and measure any ensuing absorptions with CRDS, only attempting to identify molecules responsible for absorptions coinciding with known DIBs. Subsequently, this method was used with hydrocarbon precursors alongside studies aimed at detecting specific families of molecules, such as the polar C_nH chains. Several species were observed, including a broad absorption at 5450 Å that closely matched the wavelength and FWHM of a DIB. Initially, the identity of this molecule was unknown, except that it contained only carbon and hydrogen. This absorption was subsequently attributed to the $B^1B_1 \leftarrow X^1A_1$ transition of H_2CCC (Maier *et al.* 2011a). The spectrum had been previously measured in a neon matrix by photolysis of diazopropyne (Hodges *et al.* 2006), but a slight calibration correction was required. Further gas-phase measurements using CRDS showed that the broad 5450 Å absorption correlated with the $A^1A_2 \leftarrow X^1A_1$ dipole–forbidden transition of H_2CCC in the 6150 – 6330 Å region, which had already been unambiguously identified through the observed rotational structure (Achkasova *et al.* 2006). Another broad absorption of H_2CCC was detected at 4881 Å, and a comparable DIB lies in this region, though its deconvolution is hampered by the strong H β line at 4861 Å.

Assuming the 5450 Å DIB was due to H_2CCC and using the theoretically calculated oscillator strength, a column density of 5×10^{14} cm^{-2} was inferred from the spectroscopic observations. However, such a high column density was questioned, and thus, the assignment of the 5450 Å DIB to H_2CCC (Oka & McCall 2011). A recent attempt to detect H_2CCC by mm-wave astronomy towards diffuse clouds placed an upper limit to the column density $\lesssim (1\text{–}3)\times10^{11}$ cm^{-2} (Liszt *et al.* 2012), comparable to 10^{11} cm^{-2} determined from earlier radio observations of H_2CCC in absorption (Cernicharo *et al.* 1999). The three orders of magnitude difference in column density indicates that H_2CCC cannot be the dominant contributor to the 5450 Å DIB. Nonetheless, the broad absorption at 5450 Å observed in the laboratory is that of the $B^1B_1 \leftarrow X^1A_1$ electronic transition of H_2CCC, supported by the measured anion photoelectron spectrum (Stanton *et al.* 2012). One can conclude that there must be another species with an absorption band at the same wavelength as H_2CCC and a comparable short lifetime of the excited electronic state resulting in a similar FWHM of the band.

Several factors must be considered when comparing the rotational profiles of molecules studied in the laboratory to astronomical DIB data. First, the rotational and related spectroscopic constants (e.g. spin-orbit) for both the ground and excited electronic state

have to be known. These parameters can be used to simulate line profiles at temperatures reasonable for the diffuse interstellar medium, assuming a Boltzmann distribution over the rotational states. Temperatures typically vary from around 50 – 80 K for non-polar species down to 2.7 – 10 K for polar ones. The widths of the individual rotational lines are determined by the velocity dispersion of the clouds, which is usually larger than the resolving power of the telescope used. The maximum of the unresolved profile can shift by 1 Å when changing the temperature from 10 to 100 K, as shown for the origin band of $NCCCCN^+$ in Fig. 5.

Another factor that could have an effect on rotational profiles are the weak magnetic dipole transitions in open-shell molecules with a $^2\Pi$ ground state. In this case, a non-Boltzmann population of rotational levels arises from the depopulation of the $\Omega = 1/2$ spin component to the $\Omega = 3/2$ level in the electronic ground state, i.e. the $X\,^2\Pi_{1/2} \rightarrow X\,^2\Pi_{3/2}$ transition. This effect has been considered in detail for several species, including the acetylene and diacetylene cations (Morse & Maier 2011). In diffuse clouds the rates of magnetic dipole transitions can exceed the collisional rate with hydrogen. The resulting Boltzmann rotational profiles are then somewhat distorted. A further implication of considering these types of transitions is that they may offer a means to detect non-polar molecules, such as CO_2^+ or HC_2H^+, in the mm-wave region.

Examination of the origin band of the $A\,^2\Pi_u \leftarrow X\,^2\Pi_g$ electronic transition of HC_4H^+ shows the importance of several of the aforementioned factors. This transition lies near a very weak DIB at 5069 Å (Krelowski *et al.* 2010). However, when one predicts the rotational profile, neither the shape nor the wavelength of the maximum absorption match (Maier *et al.* 2011b). This comparison is made in Fig. 8, where the top two traces show the rotational profile assuming temperatures of 30 and 60 K and a velocity dispersion of

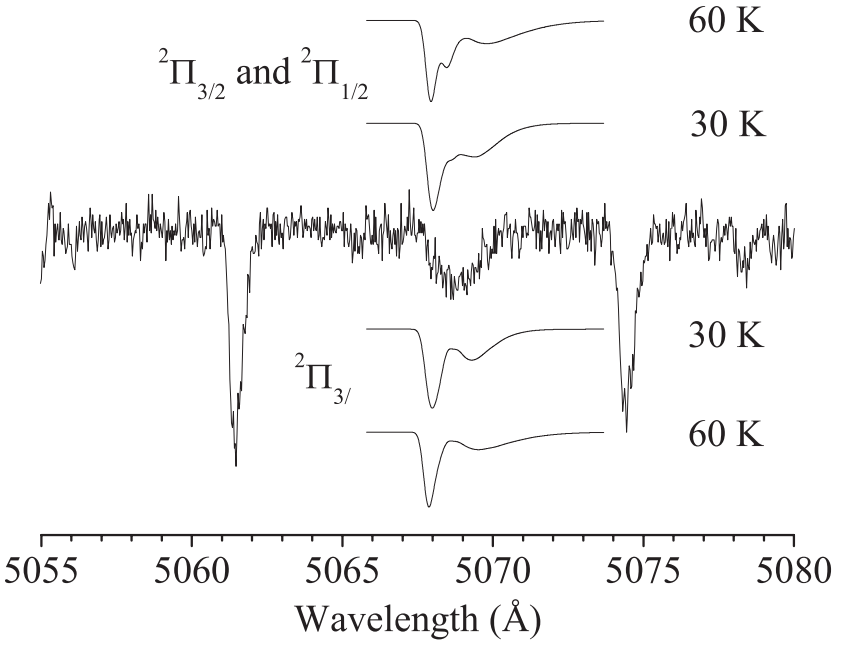

Figure 8. Rotational profiles of HC_4H^+ predicted at 30 and 60 K and assuming a Boltzmann distribution are shown in the top two traces. DIB absorptions in this region (Krelowski *et al.* 2010) are reproduced in the middle. The bottom two profiles include the effects of magnetic dipole transitions between the $\Omega = 1/2$ and $\Omega = 3/2$ spin components in the $X\,^2\Pi_g$ electronic ground state.

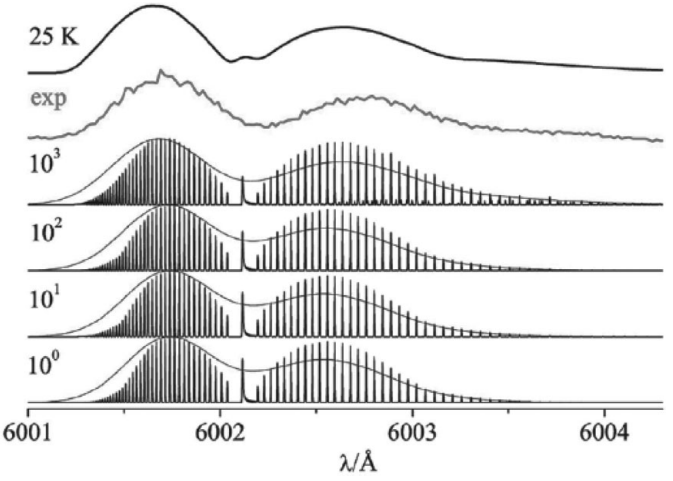

Figure 9. The simulated profile and laboratory spectrum of the HC_6H^+ $A\,^2\Pi_g \leftarrow X\,^2\Pi_u$ origin band at 25 K are shown in the top two traces, respectively. The remaining traces were generated by a collisional-radiative rate model assuming a kinetic temperature of 60 K and collisional partner density ranging from $10^0 - 10^3$ cm^{-3} (Chakrabarty *et al.* 2013).

0.33 Å; the middle trace shows the reported DIB absorptions. The difference is even more pronounced when considering the effects of this molecule's magnetic dipole transitions (bottom traces).

Further refinement can be achieved by using a collisional-radiative rate model under conditions expected in diffuse interstellar clouds. This has been done for the origin band of the $A^2\Pi_g \leftarrow X\,^2\Pi_u$ electronic transition of HC_6H^+ around 6002 Å, which was measured at 25 K by a two-color, two-photon excitation-dissociation scheme in an ion trap. The predicted profile was generated by incorporating velocity dispersion and including radiative and collisional rates, leading to a non-Boltzmann distribution (Chakrabarty *et al.* 2013). Representative data are shown in Fig. 9 where the experimental spectrum is shown along with the predicted rotational profiles for different hydrogen densities. The bottom traces show an 18 km s^{-1} velocity dispersion contour overlaid on individual J lines having a 0.007 Å FWHM.

In conclusion, new and improved laboratory methods have been used to obtain the gas-phase spectra of several potential DIB carriers, including carbon chains and rings, as well as their ions and derivatives. In conjunction with collisional-radiative rate models, these laboratory data can be compared to astronomical spectra. Clear criteria have been established for comparing laboratory and astronomical spectra, and one must ensure that line widths, rotational profiles, and wavelengths match for a definitive identification. Nonetheless, even after several decades of study and speculation, the diffuse interstellar bands remain a mystery.

Acknowledgements

The research carried out at the authors' laboratory is supported by the Swiss National Science Foundation (project 200020-140316/1) and by the European Research Council (ERC-AdG-ElecSpecIons:246998).

References

Achkasova, E., Araki, M., Densiov, A., & Maier, J. P. 2006, *J. Mol. Spectrosc.*, 237, 70

Bernstein, L. S., Clark, F. O., & Lynch, D. K. 2013, *ApJ*, 768, 84
Boguslavskiy, A. E. & Maier, J. P. 2006, *J. Chem. Phys.*, 125, 094308
Cernicharo, J., Cox, P., Fossé, D., & Güsten, R. 1999, *A&A*, 351, 341
Chakrabarty, S., Rice, C. A., Mazzotti, F. J., Dietsche, R., & Maier, J. P. 2013, *J. Phys. Chem. A*, DOI:10.1021/jp312294f
Douglas, A. E. 1977, *Nature*, 269, 130
Foing, B. H. & Ehrenfreund, P. 1994, *Nature*, 369, 296
Fulara, J., Jakobi, M., & Maier, J. P. 1993, *Chem. Phys. Lett.*, 211, 227
Hodges, J. A., McMahon, R. J., Sattelmeyer, K. W., & Stanton, J. F. 2000, *ApJ*, 544, 838
Jochnowitz, E. B. & Maier, J. P. 2008a, *Mol. Phys.*, 106, 2093
Jochnowitz, E. B. & Maier, J. P. 2008b, *Annu. Rev. Phys. Chem.*, 59, 519
Krełowski, J., Beletsky, Y., Galazutdinov, G. A., Kołos, R., Gronowski, M., & LoCurto, G. 2010, *ApJ* (Letters), 714, L64
Liszt, H., Sonnentrucker, P., Cordiner, M., & Gerin, M. 2012, *ApJ* (Letters), 753, L28
Maier, J. P., Lakin, N. M., Walker, G. A. H., & Bohlender, D. A. 2001, *ApJ*, 553, 267
Maier, J. P., Walker, G. A. H., & Bohlender, D. A. 2002, *ApJ*, 566, 332
Maier, J. P., Boguslavskiy, A. E., Ding, H., Walker, G. A. H., & Bohlender, D. A. 2006, *ApJ*, 640, 369
Maier, J. P., Walker, G. A. H., Bohlender, D. A., Mazzotti, F. J., Raghunandan, R., Fulara, J., Garkusha, I., & Nagy, A. 2011a, *ApJ*, 726, 41
Maier, J. P., Chakrabarty, S., Mazzotti, F. J., Rice, C. A., Dietsche, R., Walker, G. A. H., & Bohlender, D. A. 2011b, *ApJ* (Letters), 729, L20
McCall, B. J., York, D. G., & Oka, T. 2000, *ApJ*, 531, 329
McCall, B. J., Oka, T., Thorburn, J., Hobbs, L. M., & York, D. G. 2002, *ApJ*, 567, L145
Morse, M. D. & Maier, J. P. 2011, *ApJ*, 732, 103
Motylewski, T., Linnartz, H., Vaizert, O., Maier, J. P., Galazutdinov, G. A., Musaev, F. A., Krełowski, J., Walker, G. A. H., & Bohlender, D. A. 2000, *ApJ*, 531, 312
Nagarajan, R. & Maier, J. P. 2010, *Int. Rev. Phys. Chem.*, 29, 521
Oka, T. & McCall, B. J. 2011, *Science*, 331, 293
Rice, C. A., Rudnev, V., Dietsche, R., & Maier, J. P. 2010, *AJ*, 140, 203
Sarre, P. J., Miles, J. R., Kerr, T. H., Hibbins, R. E., Fossey, S. J., & Somerville, W. B. 1995, *MNRAS*, 277, L41
Stanton, J. F., Garand, E., Kim, J., Yacovitch, T. I., Hock, C., Case, A. S., Miller, E. M., Lu, Y-.J., Vogelhuber, K. M., Wren, S. W., Ichino, T., Maier, J. P., McMahon, R. J., Osborn, D. L., Neumark, D. M., & Lineberger, W. C. 2012, *J. Chem. Phys.*, 136, 134312
Wyss, M., Grutter, M., & Maier, J. P. 1999, *Chem. Phys. Lett.*, 304, 35